J. Fluid Mech. (2015), *vol.* 772, R1, doi:10.1017/jfm.2015.234

JFM RAPIDS
journals.cambridge.org/rapids

On damping of two-dimensional piston-mode sloshing in a rectangular moonpool under forced heave motions

O. M. Faltinsen[1,†] **and A. N. Timokha**[1,2]

[1]Centre for Autonomous Marine Operations and Systems, Department of Marine Technology, Norwegian University of Science and Technology, NO-7491, Trondheim, Norway

[2]Institute of Mathematics, National Academy of Sciences of Ukraine, 3 Tereschenkivska str., Kiev-4, 01601, Ukraine

(Received 4 February 2015; revised 12 March 2015; accepted 20 April 2015; first published online 7 May 2015)

Based on a similarity between piston-mode sloshing in a two-dimensional rectangular moonpool and a small-amplitude oscillatory flow through a slot in a slatted screen, a pressure discharge in the moonpool opening is theoretically quantified. This makes it possible, by changing the dynamic free-surface condition inside the moonpool, to account for the vortex-induced damping and thereby to modify the inviscid potential flow statement. The present paper is an important addition to Faltinsen *et al.* (*J. Fluid Mech.*, vol. 575, 2007, pp. 359–397), where a discrepancy between the potential flow theory and model tests was reported. New calculations are supported by the earlier model tests of the authors as well as numerical data obtained by means of viscous solvers.

Key words: interfacial flows (free surface), surface gravity waves, waves/free-surface flows

1. Introduction

Three- and two-dimensional piston-type resonant sloshing in moonpools (vertical openings through the decks and hulls of ships or barges) were extensively studied for about three decades – theoretically, numerically and experimentally. The focus has been on the forced vertical body oscillations without an incident wave. Faltinsen, Rognebakke & Timokha (2007) reported model tests and a semi-analytical frequency-domain solution for a linear two-dimensional rectangular moonpool problem. The high accuracy in a uniform metric was provided by a domain-decomposition method that accounts for the singular behaviour of the inviscid potential velocity field

† Email address for correspondence: odd.faltinsen@ntnu.no

at the sharp edges. The results were supported by model tests for the piston-mode resonance frequency, but the theoretical steady-state wave response was larger than in experiments. The discrepancy was explained by the vortex shedding at the sharp edges that led to non-negligible damping, which had been discussed earlier by Fukuda (1977) and Molin *et al.* (2002). This means that modelling the piston-mode sloshing requires applying a viscous solver in, at least, a domain which covers the moonpool opening. Using viscous solvers in the moonpool problem has become a popular approach in computational fluid dynamics (see e.g. Kristiansen & Faltinsen 2008; 2010; Kristiansen, Sauder & Firoozkoohi 2013; de Vries *et al.* 2013; Heo *et al.* 2014; Fredriksen, Kristiansen & Faltinsen 2015 and references therein), which has indeed produced rather good agreement with experiments.

On the other hand, adopting viscous solvers may, generally speaking, make the computational procedures time-consuming; therefore, when the task is a parameter study, the moonpool problem continues to be solved by semi-analytical methods, normally those based on the inviscid potential flow statement (Zhang & Bandyk 2013; Zhou 2013; Zhou, Wu & Zhang 2013; Liu & Li 2014; McIver 2014). As discussed by Molin *et al.* (2002, 2009), Faltinsen *et al.* (2007) and Faltinsen & Timokha (2009), this statement could be successfully modified to account for the vortex-induced damping by quantifying the pressure discharge in the moonpool opening. The principal difficulty is that the pressure discharge (drop) coefficient is unknown *a priori*. An important question is: how can this coefficient be estimated without conducting dedicated model tests? The authors had no good idea in 2006–2007 when working on the paper Faltinsen *et al.* (2007).

In 2010–2011, Faltinsen, Firoozkoohi & Timokha (2011) successfully studied the liquid sloshing dynamics in a tank with a slatted screen, where an analogous pressure discharge condition was employed to modify the inviscid potential flow model. Flows through such screens are well studied experimentally, and there are various empirical formulas, tables and relations (see e.g. Blevins 1992) representing, for oscillatory motions, the pressure drop coefficient K as a function of the screen shape, solidity ratio Sn and Keulegan–Carpenter number K_c.

In the present paper (which could be considered an extra section of Faltinsen *et al.* 2007), by making use of a similarity we discovered between the piston-mode sloshing in a two-dimensional rectangular moonpool and oscillatory flows through a slot in a slatted screen, we determine artificial Sn and K_c values and, by applying a known dependence $K = K(Sn, K_c)$ for screens, quantify the pressure discharge in the moonpool opening. By incorporating the pressure discharge condition into the statement of Faltinsen *et al.* (2007) (so that the dynamic free-surface condition in the moonpool opening is modified) and the solution method, we recompute the aforementioned steady-state wave response. The new results are supported by our previous model tests and by the numerical viscous solutions obtained in Kristiansen & Faltinsen (2008, 2012).

2. Statement

Following Faltinsen *et al.* (2007), we consider two-dimensional $O\bar{z}$-symmetric steady-state surface waves excited by small-amplitude vertical harmonic motions of two rigidly connected rectangular hulls, $\eta_3(t) = -\eta_{3a}\cos(\sigma t)$, in finite-depth water as shown in figure 1(*a*). The potential inviscid motions of incompressible liquid are assumed. The non-dimensional statement takes the gap width L_1 as the characteristic

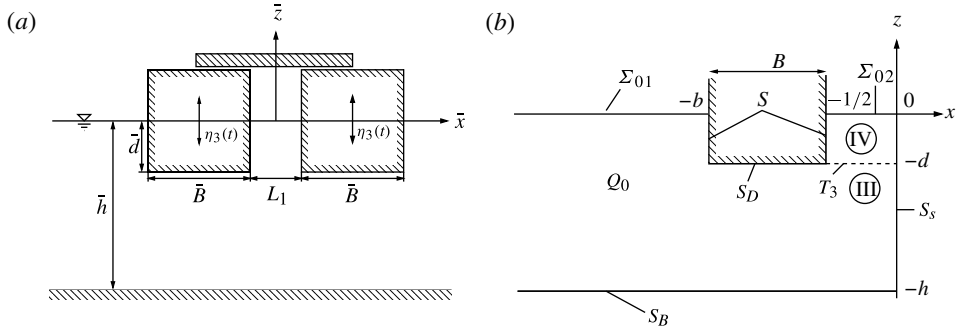

FIGURE 1. Sketch of (*a*) the dimensional moonpool and (*b*) the left part of the L_1-scaled symmetric liquid domain.

dimension and $1/\sigma$ as the characteristic time. This leads to the non-dimensional variables

$$x=\frac{\bar{x}}{L_1},\quad z=\frac{\bar{z}}{L_1},\quad t=\sigma\bar{t},\quad \Lambda=\frac{\sigma^2 L_1}{g},\quad \psi(x,z,t)=\frac{\bar{\psi}(\bar{x},\bar{z},\bar{t})}{L_1^2\sigma},\quad p(x,z,t)=\frac{\bar{p}(\bar{x},\bar{z},\bar{t})}{\rho g L_1} \tag{2.1a–f}$$

(with the dimensional variables marked by an overbar), where g is the gravity acceleration, $\psi(x, z, t)$ and $p(x, z, t)$ are the non-dimensional velocity potential and pressure, respectively, ρ is the liquid density, g is the gravitational acceleration and $\epsilon=\eta_{3a}/L_1\ll 1$. As a consequence, the distance between the rectangular bodies and the Oz-axis becomes $1/2$, the non-dimensional water depth is $h=\bar{h}/L_1$, and the scaled dimensions of the stationary immersed rectangular body are $d=\bar{d}/L_1$ in the vertical (draft) direction and $B=\bar{B}/L_1=\bar{b}/L_1-1/2$ in the horizontal direction. The left normalized liquid domain is shown in figure 1(*b*).

At a certain forcing frequency σ_* (non-dimensional $\Lambda_*=\sigma_*^2 L_1/g$ by (2.1)), a resonant piston-mode sloshing occurs between the hulls. The inviscid potential flow statement well predicts Λ_*, which can be computed using the method of Faltinsen *et al.* (2007), for example, or approximated by the formula of Molin (2001). When deriving the latter formula, Molin artificially extended the rectangular hulls left and right to infinity but inserted two sinks at $\pm b_*$ (with $b_*>b$) on the extended hull bottom. The b_* value is unknown *a priori*. When taking $b_*=b$, the Molin formula gives a rough prediction of Λ_*. However, if we already know Λ_* (computed by another method), we can find

$$b_*=2\exp\left((\Lambda_*^{-1}-d)\pi-\tfrac{3}{2}\right)>b \tag{2.2}$$

by inverting the formula (see equation (4.12) in Faltinsen *et al.* 2007). Molin's solution will then give an approximation of the resonant piston-mode flows in the vicinity of the opening. Far from the opening, this approximation fails since it is assumed that there are no free-surface waves at infinity.

Figure 2 gives a schematic comparison of the local (at the opening) Molin's piston-type sloshing (panel *b*) and an oscillatory steady-state flow through a slot in the slatted screen with a uniform (non-dimensional) harmonic approach velocity of $U(t)$ (panel *a*). The free surface in (*b*) remains far from the edges (provided by a finite draft d) so that the liquid flux per half-period is much less than the mean liquid volume inside the opening. Looking for a similarity in (*a*) implies the same

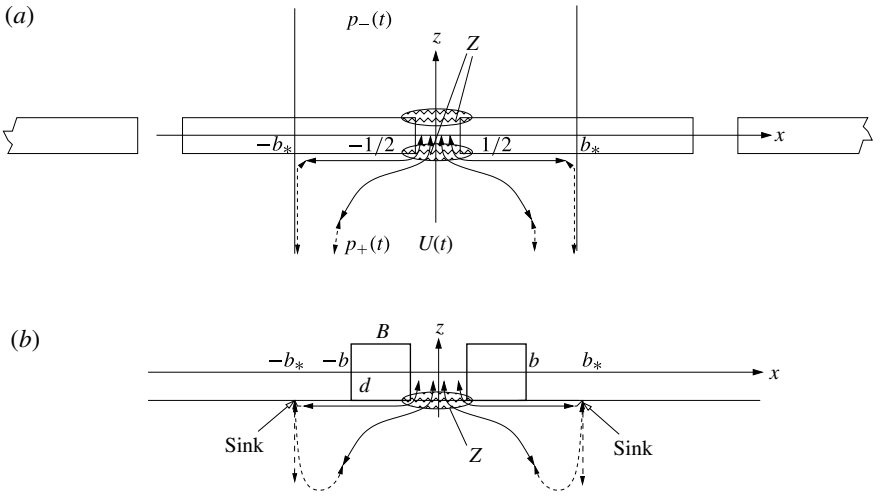

FIGURE 2. Simplified schematic representations of: (*a*) small-amplitude oscillatory steady-state liquid motions through a slot of a slatted screen; (*b*) piston-mode sloshing in a rectangular moonpool according to the approximation of Molin (2001). The latter implies artificial sinks at $(\pm b_*, -d)$ and an extended solid hull bottom for $b < |x|$, $z = -d$. Fluid particles do not cross the lines $x = \pm b_*$, $z < -d$ and $b_* < |x| < b$, $z = -d$ (excluding ends). Within the framework of our averaged pressure discharge approach, the vortex shedding from the sharp edges is assumed to be located mainly in zones Z (i.e. two zones and one zone in cases (*a*) and (*b*), respectively). Dashed streamline components mark differences between (*a*) and (*b*) that disappear as the opening is approached, i.e. when $z \to -d, z < -d$ and $-b_* < x < b_*$.

for the liquid flux through a single slat, which is only possible for relatively small flux-velocity amplitudes and non-small slat thicknesses $2d$. One can then introduce a fictitious almost-flat interface in the slot between the upper and lower liquid domains. The interface oscillates about the mean level $z = 0$ and remains far away from the edges. The lower/upper liquid flow (separated by this interface) displays a similarity to the piston-type sloshing. Streamlines are shown by solid and dashed lines, with the solid lines demonstrating the flow similarity close to the openings. The flow separates at the inlet to the moonpool and at the outlet/inlet of the screen opening. We simplify the details of the vorticity field due to flow separation by locating it principally in zones Z. Our primary objective is to express the consequence of flow separation in terms of a space-averaged (mean) pressure discharge across the moonpool without giving details on the vorticity field, which can in reality be rather complicated.

For the screen flow in figure 2(*a*), there is an analogy to b_* at the middle of the slat, implying no cross-flows through the vertical lines $x = \pm b_*$ which confine the liquid flux through the chosen central slot. The solidity ratio is defined via b_* as $Sn = (2b_* - 1)/(2b_*)$. If $u_0(t)$ is the mean non-dimensional vertical (flux) velocity through the slot, i.e. $u_0(t) = \int_{-1/2}^{1/2} v(x, t)\,\mathrm{d}x$, then the harmonic non-dimensional approach velocity can be expressed as $U(t) = u_0(t)/(2b_*)$ and the Keulegan–Carpenter number as $K_c = 2\pi\bar{U}_a/(2\sigma\bar{b}_*) = \pi u_{0a}/(2b_*^2)$, where the overbars imply dimensional values, $\bar{U}_a = \bar{u}_{0a}/(2\bar{b}_*)$ (the dimensional amplitude of $\bar{U}(t)$) and $u_{0a} = 2\bar{b}_*\bar{U}_a/(L_1^2\sigma)$ is the non-dimensional amplitude. When following standard definitions, the spatial mean

pressure discharge between the upper (–) and lower (+) liquid domains at each slot of the slatted screen is

$$\Delta\bar{p} = \bar{p}_+(t) - \bar{p}_-(t) = \frac{1}{2}\rho K(Sn, K_c)\bar{U}(t)|\bar{U}(t)|$$
$$= \frac{1}{8b_*^2}\rho K\left(\frac{2b_*-1}{2b_*}, \frac{\pi u_{0a}}{2b_*^2}\right)\bar{u}_0(t)|\bar{u}_0(t)|, \tag{2.3a}$$

$$\Delta p = p_+(t) - p_-(t) = \frac{1}{8b_*^2}\Lambda K\left(\frac{2b_*-1}{2b_*}, \frac{\pi u_{0a}}{2b_*^2}\right)u_0(t)|u_0(t)| \tag{2.3b}$$

(see equation (15) in Faltinsen *et al.* 2011) in the dimensional and non-dimensional (according to (2.1)) statements, respectively, where ρ is the liquid density. The right-hand side of (2.3) shows that the pressure discharge depends on the mean flux velocity. Faltinsen *et al.* (2011) demonstrated that, for sloshing problems, dealing with a complex non-uniform approach velocity field keeps the formulas applicable when these are based on the flux velocity $u_0(t)$.

Figure 2(*b*) schematically shows small-amplitude oscillatory flows associated with the piston-mode sloshing in a rectangular moonpool within the approximation framework of Molin (2001) and compares them with those in figure 2(*a*). In both cases, liquid particles have zero horizontal velocity component along the lines $x = \pm b_*$, $y < -d$ and $b < |x| < b_*$, $z = -d$. In other words, the particles do not cross the vertical lines due to a symmetry (in the case of *a*) and because of the sinks at $x = \pm b_*$ (in the case of *b*), causing the particles to move along these lines. A difference is that liquid comes from infinity in case (*a*) but there are two sinks in case (*b*) and, as a consequence, the dashed streamline components do not coincide. However, the dashed streamline components disappear when approaching the structures (without ends), i.e. $z \to -d$, $z < -d$ and $-b_* < x < b_*$; therefore, one can say that the local velocity fields are similar at the openings (only solid streamline parts appear there). Moreover, the total liquid flux through the openings on $-1/2 < x < 1/2$ (or through the structure for $-b_* < x < b_*$, without ends) is also determined by the same integral, $u_0(t) = \int_{-1/2}^{1/2} v(x, t)\,\mathrm{d}x$. Accounting for this local similarity (close to the openings) implies that the meanings of $Sn = (2b_* - 1)/(2b_*)$ and $K_c = \pi u_{0a}/(2b_*^2)$ look similar in cases (*a*) and (*b*). Thus, if we know the function $K = (Sn, K_c)$ for the screen case (*a*), we can use it to describe the pressure discharge in the moonpool opening IV – within the 1/2 multiplier in (2.3*b*) since case (*b*) is characterized by a single zone *Z*: $\Delta p(t)|_{moonpool} = \Delta p(t)/2$.

The following equation and boundary conditions with respect to $\psi(x, z, t)$ remain unchanged and can be taken from Faltinsen *et al.* (2007) (see the notation in figure 1*b*):

$$\nabla^2\psi = 0 \quad \text{in } Q_0, \qquad \frac{\partial\psi}{\partial n} = 0 \quad \text{on } S_B + S + S_S, \qquad \frac{\partial\psi}{\partial z} = \epsilon\sin t \quad \text{on } S_D, \tag{2.4a–c}$$

$$\Lambda\frac{\partial^2\psi}{\partial t^2} + \frac{\partial\psi}{\partial z} = 0 \quad \text{on } \Sigma_{01}, \tag{2.5}$$

$$\psi \sim F(\mathscr{K}x + t, z) \quad \text{as } x \to -\infty, \qquad \psi(x, z, t + 2\pi) \equiv \psi(x, z, t), \tag{2.6a,b}$$

where Σ_{01} is the unperturbed free surface outside the moonpool opening, S represents the mean wetted vertical walls of the stationary rectangle, S_B is the horizontal

seabed, S_D is the bottom of the rectangular body, S_S is the artificial vertical wall caused by the Oz-symmetry and n is the outer normal to the fluid boundary. The periodicity condition at infinity in (2.6) implies that we look for the steady-state periodic solution. The wavenumber $\mathscr{K}$ and function F are unknown and should be found together with ψ.

Within the framework of our averaging pressure discharge technique, $\Delta p(t)|_{moonpool}$ occurs at the keel level T_3, i.e. between domains III and IV in figure 1(*b*). It leads to a time-dependent jump of the velocity potential which can be excluded (making ψ continuous at T_3) via the standard substitution $\psi|_{IV} := \psi|_{IV} + C(t)$ with appropriate $C(t)$. Derivations show that by proceeding in this way one changes the linear dynamic free-surface condition on Σ_{02}:

$$\Lambda\frac{\partial\psi}{\partial t}+f=\boxed{\frac{1}{16b_*^2}\Lambda_* K\left(\frac{2b_*-1}{2b_*},\frac{\pi u_{0a}}{2b_*^2}\right)u_0(t)|u_0(t)|}\quad\text{where}\quad\frac{\partial\psi}{\partial z}=\frac{\partial f}{\partial t}\qquad(2.7)$$

is the kinematic condition (which remains unchanged) on Σ_{02}, with $z=f(x,t)$ defining the free-surface elevation and with the x-averaged flux velocity given by

$$u_0(t)=2\int_{-1/2}^{0}\frac{\partial\psi}{\partial z}(x,-d,t)\,\mathrm{d}x-\epsilon\sin t,\qquad u_{0a}=\max_{0\leqslant t<2\pi}|u_0(t)|.\qquad(2.8a,b)$$

Because we construct the theory to be applicable in a neighbourhood of Λ_*, we use Λ_* instead of Λ in front of the nonlinear term in (2.7).

The difference between (2.4)–(2.8) and the standard free-surface problem (see Faltinsen *et al.* 2007) lies in the framed nonlinear integral term in the dynamic free-surface condition (2.7). A similar modified dynamic free-surface condition was used by Molin *et al.* (2009) ('fictitious plate model') and Newman (2003) ('lid methods'). Our statement suggests that we know *a priori* the non-dimensional resonant frequency Λ_*, that b_* is computed from (2.2) and that Λ is close to Λ_*. Obtaining Λ_* implies finding Λ for which the maximum wave response of (2.4)–(2.8) occurs without the framed term.

3. Numerical steady-state solution

Suggesting the equivalent linearization method, we will focus on finding the $\cos t$ and $\sin t$ harmonic components of the steady-state solution of (2.4)–(2.8). Supplementary materials (available at http://dx.doi.org/10.1017/jfm.2015.234) provide analytical and numerical details of the method of Faltinsen *et al.* (2007) and present its modifications due to the extra nonlinear quantity in (2.7). We adopt the Baines–Peterson–Weisbach formula (Weisbach 1855; Baines & Peterson 1951)

$$K=K(Sn)=\left(\frac{1}{C_0(1-Sn)}-1\right)^2,\qquad C_0=0.405\exp(-\pi Sn)+0.595,\qquad(3.1a,b)$$

which expresses the pressure drop coefficient as a function of $Sn>0.3$ (controlled in numerical examples). The formula assumes that K does not depend on the Keulegan–Carpenter number K_c. Faltinsen *et al.* (2011) successfully applied it to study sloshing in a screen-equipped tank. Improvement of (3.1) to include the K_c effect was recently discussed by Hamelin *et al.* (2013).

Comparisons of our new computations (solid lines) with experimental measurements (empty symbols) and nonlinear viscous simulations (filled symbols) are presented in

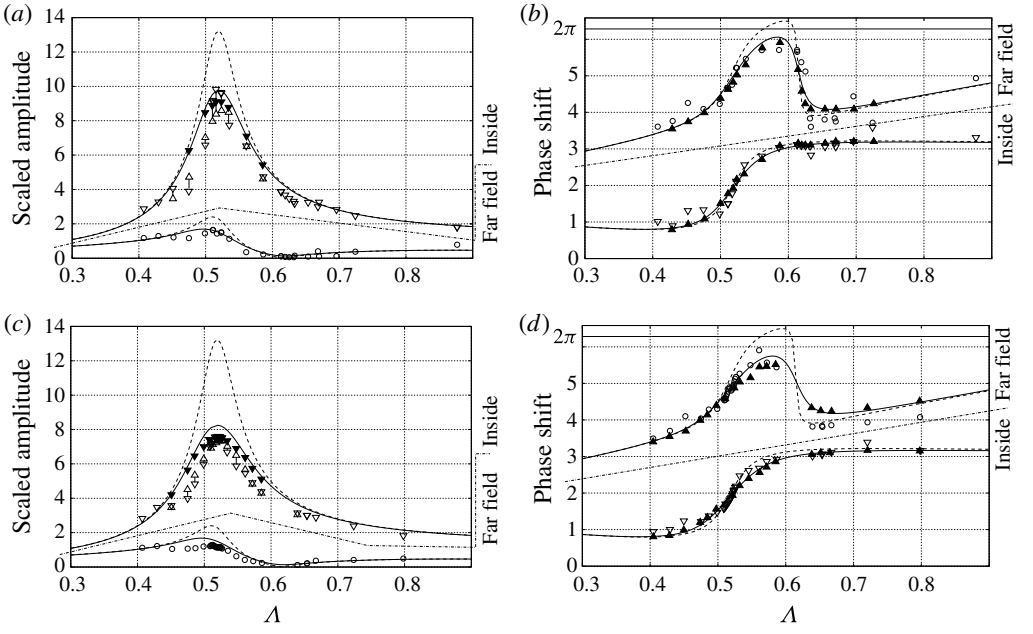

FIGURE 3. Experimental case 1 of Faltinsen *et al.* (2007) ($B = 1$, $d = 1$ and $h = 5.72222$): (a,c) theoretical and experimental maximum wave elevations of the piston-mode sloshing and the maximum wave elevations at $x = w11 = 3.88889$, scaled by the forcing amplitude; (b,d) the corresponding phase shifts relative to the input sinusoidal motions of the hulls. In all panels the amplitude and phase results are plotted against Λ, for a non-dimensional forcing amplitude of (a,b) $\epsilon = 0.013889$; (c,d) $\epsilon = 0.027778$. The experimental data are taken from Faltinsen *et al.* (2007): $\triangle$, the measured maximum steady-state wave elevations inside the moonpool opening in (a,c) and the corresponding phase shifts in (b,d); $\bigcirc$, the measured maximum wave elevations and phase shifts at $x = 3.88889$; $\triangledown$, the measured maximum elevations inside the opening filtered against the reflection effect of the outgoing wave (Kristiansen & Faltinsen 2008). The dashed lines are taken from Faltinsen *et al.* (2007) and represent the inviscid potential flow prediction. The solid lines represent our computations accounting for the $\sin t$ and $\cos t$ harmonics. Other numerical results are marked by filled triangles; they are taken from Kristiansen & Faltinsen (2008), who used a vortex-tracking model to account for the vortex-shedding effect at the lower moonpool edges.

figures 3–6. In addition, the dashed lines denote numerical results from Faltinsen *et al.* (2007). We focus on the maximum wave amplitude inside the moonpool opening, the maximum steady-state wave elevations far from the hulls (at the control point $x = w11$) and the corresponding phase shifts (with respect to the $\sin t$ forcing). More details on the experimental cases, viscous solvers and notation used can be found in Faltinsen *et al.* (2007), Kristiansen & Faltinsen (2008, 2012) and Fredriksen *et al.* (2015).

Figure 3 focuses on the experimental case 1 of Faltinsen *et al.* (2007), where, under the same geometric input parameters, two different forcing amplitudes were tested. The caption explains the notation used. One should note that the measured maximum wave elevation inside the moonpool opening is, according to Kristiansen & Faltinsen (2008), affected by the wave reflection from a wall in the experimental wave basin. Other measurements, namely the maximum wave elevation at $w11$ and the phase shifts, were virtually uninfluenced by the reflection. Thus, along with symbols

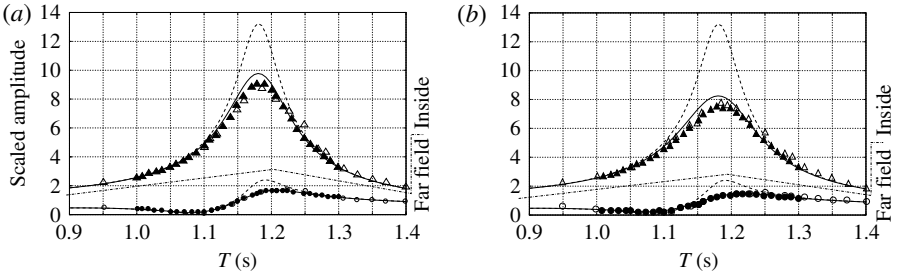

FIGURE 4. Same as figure 3(*a*,*c*) except that the comparison is with experimental data reported by Kristiansen & Faltinsen (2012) (empty symbols). Following the original experimental publication, the amplitude and phase-shift results are plotted against the dimensional forcing period T. The solid symbols show the numerical results of Kristiansen & Faltinsen (2012), obtained by applying a viscous solver to the liquid domain in the vicinity of the hulls: ▲, maximum wave elevation; ●, phase shift.

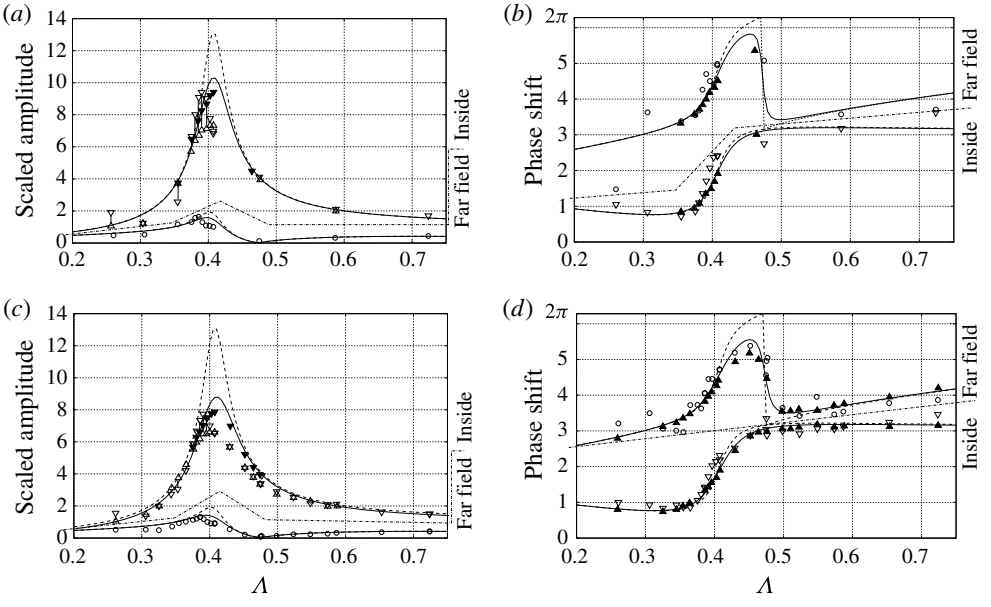

FIGURE 5. Same as figure 3 but for the experimental case 2 of Faltinsen *et al.* (2007) (with $d = 1.5$).

△ representing the actual measurements of maximum wave elevation in the moonpool opening, we have introduced inverted symbols ▽ to denote filtered output signals that are believed not to be affected by the reflection. Furthermore, Kristiansen & Faltinsen (2008) conducted nonlinear simulations that accounted for the vortex shedding at the sharp lower edges of the rigid hulls. Their numerical results are shown by filled triangles: the symbols ▼ represent numerical maximum wave elevations inside the moonpool opening, and the symbols ▲ mark numerical results for the phase shifts. What we see from the figure is that our new theoretical results are in satisfactory agreement with both the experiments and the computations of Kristiansen & Faltinsen (2008).

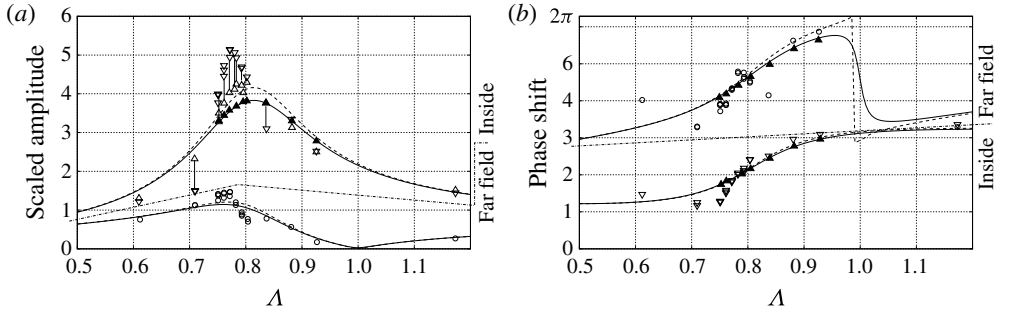

FIGURE 6. Same as in figure 3 but for the experimental case 3 of Faltinsen *et al.* (2007) ($B = 1$, $d = 0.5$, $h = 2.86111$, $\epsilon = 0.006944$ and $w11 = 1.94444$).

Kristiansen & Faltinsen (2012) reported additional (control) model tests with the same geometrical and physical input parameters as in case 1 of Faltinsen *et al.* (2007). These model tests aimed at minimizing the aforementioned reflection effect. Kristiansen & Faltinsen (2012) also proposed a domain-decomposition method which suggests applying a nonlinear viscous solver to the fluid domain in the vicinity of the hull. We compare our theoretical output (solid lines) with the inviscid potential flow solution (dashed lines) and these additional experimental and viscous numerical results in figure 4. We see that our new approximation of the steady-state solution agrees satisfactorily with both experimental and numerical values.

To complete the validation procedure, we compare our new theoretical predictions with experimental cases 2 and 3 from Faltinsen *et al.* (2007) in figures 5 and 6. Again, our approximation shows satisfactory agreement with the model tests and the nonlinear simulations by Kristiansen & Faltinsen (2008), especially for case 3.

4. Conclusions

Describing the piston-mode resonant sloshing in a moonpool may involve inviscid potential flow solvers (see Zhang & Bandyk 2013; Zhou 2013; Zhou *et al.* 2013; Liu & Li 2014; McIver 2014 and references therein), which give an accurate prediction of the resonant frequencies but, unfortunately, overpredict the steady-state resonant response. One reason for this discrepancy is the damping due to the vortex shedding at the lower moonpool edges. Getting an accurate theoretical prediction of the resonance response involves using viscous solvers in the liquid domain in the vicinity of the hull. Kristiansen & Faltinsen (2008, 2012) and Fredriksen *et al.* (2015) (two-dimensional moonpool), Kristiansen *et al.* (2013) (three-dimensional moonpool) and many other authors have proposed appropriate solvers. However, the inviscid potential flow model remains popular when the main task is a parameter study and employing the viscous solvers may be non-efficient. Following Molin *et al.* (2002, 2009) and Newman (2003), one could introduce the pressure discharge condition in the cross-section of the moonpool opening to improve the inviscid statement. The problem consists of estimating the pressure drop coefficient without performing dedicated model tests. Such an estimation is proposed in the present paper for finite draft-to-opening-width ratios based on a similarity between small-amplitude harmonic flows through a slot of a slatted screen and the approximation of Molin (2001) for the piston-mode sloshing in a rectangular moonpool. Comparing our numerical results with the experimental

data of Faltinsen *et al.* (2007) and numerical results from Kristiansen & Faltinsen (2008, 2012) showed satisfactory agreement. This validates our estimate.

Our analysis deals with the two-dimensional rectangular moonpool. We believe that it can be generalized to other moonpool shapes, including three-dimensional ones, provided that: (i) the moonpool walls away from a local edge zone (associated with Z in figure 2) are vertical, so that the Ox-symmetry projection of the moonpool opening in figure 2(*b*) yields the corresponding fictitious slot shape in figure 2(*a*); (ii) the empirical function $K = K(Sn, K_c)$ exists for this fictitious slot shape; and (iii) Molin's formula (Molin 2001; Molin *et al.* 2009) can be generalized to the needed moonpool shape. For the three-dimensional case, condition (iii) is the most difficult one, since generally speaking one should operate with a curve instead of a single number b_*, and the multiplicity of the resonant frequencies matters. A dedicated study should be conducted to find more precise formulas $K = K(Sn, K_c)$ that reflect the K_c effect and to validate them by using empirical values of K established in experiments (e.g. by Molin *et al.* 2009). Another requirement (or limitation) consists of having an inviscid potential solver for the modified problem (2.4)–(2.8). The solver can be based on either a semi-analytical scheme of Faltinsen *et al.* (2007) type or boundary/finite element algorithms (see e.g. Uzair & Koo 2012; Feng & Bai 2015).

It also remains to generalize the procedure to a free-floating body with a moonpool in incident waves. This was done experimentally and numerically with a combined potential flow and near-field viscous flow solver by Fredriksen *et al.* (2015) for a similar two-dimensional section. In that case, the maximum piston-mode oscillations occur not at the piston-mode resonance frequency but at a nearby heave resonance frequency caused by the presence of the moonpool.

Acknowledgements

This research was carried out at the Centre for Autonomous Marine Operations and Systems (AMOS); the Norwegian Research Council is acknowledged as the main sponsor of AMOS. This work was supported by the Research Council of Norway through the Centres of Excellence funding scheme, project number 223254 – AMOS.

Supplementary data

Supplementary data available at http://dx.doi.org/10.1017/jfm.2015.234.

References

BAINES, W. D. & PETERSON, E. G. 1951 An investigation of flow through screens. *ASME Trans.* **73**, 467–479.

BLEVINS, R. D. 1992 *Applied Fluid Dynamics*. Krieger.

FALTINSEN, O. M., FIROOZKOOHI, R. & TIMOKHA, A. N. 2011 Steady-state liquid sloshing in a rectangular tank with a slat-type screen in the middle: quasi-linear modal analysis and experiments. *Phys. Fluids* **23**, 042101.

FALTINSEN, O. M., ROGNEBAKKE, O. F. & TIMOKHA, A. N. 2007 Two-dimensional resonant piston-like sloshing in a moonpool. *J. Fluid Mech.* **575**, 359–397.

FALTINSEN, O. M. & TIMOKHA, A. N. 2009 *Sloshing*. Cambridge University Press.

FENG, X. & BAI, W. 2015 Wave resonances in a narrow gap between two barges using fully nonlinear numerical simulation. *Appl. Ocean Res.* **50**, 119–129.

FREDRIKSEN, A. G., KRISTIANSEN, T. & FALTINSEN, O. M. 2015 Wave-induced response of a floating two-dimensional body with a moonpool. *Phil. Trans. R. Soc. Lond.* A **373** (2033), 20140109.

FUKUDA, K. 1977 Behaviour of water in vertical well with bottom opening of ship, and its effect on ship motions. *J. Soc. Nav. Archit. Japan* **141**, 107–122.

HAMELIN, J. A., LOVE, J. S., TAIT, M. J. & WILSON, J. C. 2013 Tuned liquid dampers with a Keulegan–Carpenter number-dependent screen drag coefficient. *J. Fluids Struct.* **43**, 271–286.

HEO, J.-K., PARK, J.-C., KOO, W.-C. & KIM, M.-H. 2014 Influences of vorticity to vertical motion of two-dimensional moonpool under forced heave motion. *Math. Probl. Engng* **2014**, 423927.

KRISTIANSEN, T. & FALTINSEN, O. M. 2008 Application of a vortex tracking method to the piston-like behaviour in a semi-entrained vertical gap. *Appl. Ocean Res.* **30**, 1–18.

KRISTIANSEN, T. & FALTINSEN, O. M. 2010 A two-dimensional numerical and experimental study of resonant coupled ship and piston-mode motion. *Appl. Ocean Res.* **32**, 158–176.

KRISTIANSEN, T. & FALTINSEN, O. M. 2012 Gap resonance analyzed by a new domain-decomposition method combining potential and viscous flow draft. *Appl. Ocean Res.* **34**, 198–208.

KRISTIANSEN, T., SAUDER, T. & FIROOZKOOHI, R. 2013 Validation of a hybrid code combining potential and viscous flow with application to 3D moonpool. In *Proceedings of the ASME 2013 32nd International Conference on Ocean, Offshore and Arctic Engineering (OMAE2013), June 9–14, 2013, Nantes, France*, vol. 12. American Society of Mechanical Engineers.

LIU, Y. & LI, H.-J. 2014 A new semi-analytical solution for gap resonance between twin rectangular boxes. *Proc. Inst. Mech. Engrs, Part M* **228**, 3–16.

MCIVER, P. 2014 An extended wide-spacing approximation for two-dimensional water-wave problems in infinite depth. *Q. J. Mech. Appl. Maths* **67** (3), 445–468.

MOLIN, B. 2001 On the piston and sloshing modes in moonpools. *J. Fluid Mech.* **430**, 27–50.

MOLIN, B., REMY, F., CAMHI, A. & LEDOUX, A. 2009 Experimental and numerical study of the gap resonances in-between two rectangular barges. In *Proceedings of the 13th Congress of the International Maritime Association of the Mediterranean (IMAM 2009), 12–15 October, Istanbul, Turkey*.

MOLIN, B., REMY, F., KIMMOUN, O. & STASSEN, Y. 2002 Experimental study of the wave propagation and decay in a channel through a rigid ice-sheet. *Appl. Ocean Res.* **24** (5), 5–20.

NEWMAN, J. N. 2003 Application of generalized modes for the simulation of free surface patches in multiple body interactions. *Tech. Rep.* WAMIT Consortium.

UZAIR, A. S. & KOO, W. 2012 Hydrodynamic analysis of a floating body with an open chamber using a 2D fully nonlinear numerical wave tank. *Intl J. Nav. Archit. Ocean Engng* **4**, 281–290.

DE VRIES, I., ROUX, Y., NACIRI, M. & BONNAFFOUX, G. 2013 Dynamics of entrapped water in large turret moonpools. In *Proceedings of the ASME 2013 32nd International Conference on Ocean, Offshore and Arctic Engineering (OMAE2013), June 9–14, 2013, Nantes, France*, paper no. OMAE2013-11467. American Society of Mechanical Engineers.

WEISBACH, J. 1855 *Die Experimental Hydraulik*. J. G. Engelhardt.

ZHANG, X. & BANDYK, P. 2013 On two-dimensional moonpool resonance for twin bodies in a two-layer fluid. *Appl. Ocean Res.* **40**, 1–13.

ZHOU, H.-W. 2013 Radiation and diffraction analysis of a cylindrical body with a moon pool. *J. Hydrodyn.* **25** (2), 196–204.

ZHOU, H. W., WU, G. X. & ZHANG, H. S. 2013 Wave radiation and diffraction by a two-dimensional floating rectangular body with an opening in its bottom. *J. Engng Maths* **83**, 1–22.